Axisymmetric Static and Dynamic Buckling of Orthotropic Shallow Conical Caps

P. C. Dumir* and K. N. Khatri†
Indian Institute of Technology, New Delhi, India

This study deals with the axisymmetric static and dynamic buckling of elastic polar orthotropic thin shallow conical caps subjected to uniformly distributed loads. Static and step function conservative loadings on conical caps with clamped immovable, simply supported immovable, and simply supported movable edges have been considered. The governing equations are formulated in terms of normal displacement w and stress function ψ. Orthogonal point collocation method is used for spatial discretization and Newmark-β scheme is used for time marching. The present results for the isotropic clamped immovable conical caps are in good agreement with the available results. The influence of orthotropic parameter β and the edge conditions on the static and dynamic buckling loads has been investigated. Dynamic buckling loads obtained from static analysis have been found to agree well with the dynamic buckling loads based on transient response.

Nomenclature

a = radius of base of the cap
a_i, b_i = coefficients of power series expansions of w and ψ
A_1, A_2, A_3 = coefficients in quadratic extrapolation
D = $E_\theta h^3/[12(\beta - \nu_\theta^2)]$
E = minimum of E_r and E_θ
E_r, E_θ = elastic moduli
h = thickness of the cap
H = apex height
M_r, M_θ = bending moments
N, ρ_i = number and radii of collocation points
N_r, N_θ = in-plane forces
p_{CL} = classical buckling pressure for isotropic full spherical shell with Young's modulus E and Poisson's ratio ν
q = uniformly distributed load over the entire cap
Q = nondimensional load, $= \frac{1}{8}[3(1-\nu^2)]^{\frac{1}{2}}(h/H)^2(qa^4/Eh^4)$
Q_{cr} = buckling loads
Q_r = transverse shear
r, ρ = radius, nondimensional radius
t, τ = time, nondimensional time
u^*, w^* = in-plane and normal displacements
$\bar{w}, \bar{w}_{\max}$ = average deflection, maximum average deflection
w_0^* = initial position of the middle surface above the base
β = orthotropic parameter, $= E_\theta/E_r = \nu_\theta/\nu_r$
γ = mass density
$\Delta\tau$ = time step size
$\epsilon_{\gamma,\theta}$ = strains
ν = maximum of ν_r and ν_θ
ν_r, ν_θ = Poisson's ratios
$\sigma^*_{\gamma,\theta}$ = stresses
ψ^*, ψ = stress function, nondimensional stress function

Superscripts
$(\,)', (\dot{\ })$ = partial derivatives with respect to ρ and τ

Subscripts
J = marching step
p = predicted value
i = value at the ith collocation point
$,r; ,t$ = partial derivatives with respect to r and t

Received Feb. 12, 1984; revision received Nov. 26, 1984.

*Assistant Professor, Department of Applied Mechanics.
†Graduate Student, Department of Applied Mechanics.

Introduction

NONLINEAR static and dynamic buckling of elastic shallow caps have received great attention[1] due to their importance in the area of aerospace and mechanical engineering. Most of the investigations consider the case of shallow spherical caps. Deep conical shells have been extensively studied, but shallow conical shells have received little attention. Akkas and Bauld[2,3] used finite difference techniques to analyze the static and dynamic buckling behavior of clamped isotropic shallow conical shells under uniformly distributed loads and a point load at the apex. Hubner and Emmerling[4] and Hubner[5] have presented the static response of isotropic shallow truncated conical caps with a free hole under an axial central load.

The object of this investigation is to study the axisymmetric static and dynamic buckling of elastic cylindrically orthotropic thin shallow conical caps subjected to uniformly distributed loads normal to the undeformed surface over the entire cap. Static and step function conservative loads have been analyzed. Conical caps with clamped immovable, simply supported immovable, and simply supported movable edges have been considered. The influence of orthotropic parameter β and the edge conditions on the static and dynamic buckling loads have been investigated. Dynamic buckling loads have also been obtained from static analysis and have been found to agree well with the results obtained from the forced vibration analysis.

Mathematical Formulation

Marquerre-type governing equations for axisymmetric moderately large deflection of cylindrically orthotropic shallow conical shell are formulated in terms of normal displacement w and stress function ψ. The middle surface of a conical cap of base radius a and apex rise H (Fig. 1) is given by

$$w_0^* = H[1 - (r/a)] \tag{1}$$

The constitutive equations for cylindrical orthotropy and the strain displacement relations for moderately large axisymmetric deflections of shallow caps are

$$\epsilon_r = u^*_{,r} - w^*_{0,r} w^*_{,r} + \frac{1}{2} w^{*2}_{,r} - z w^*_{,rr} = \frac{\sigma^*_r}{E_r} - \nu_\theta \frac{\sigma^*_\theta}{E_\theta}$$

$$\epsilon_\theta = \frac{u^*}{r} - \frac{z}{r} w^*_{,r} = \frac{\sigma^*_\theta}{E_\theta} - \nu_r \frac{\sigma^*_r}{E_r} \tag{2}$$

with $\beta = E_\theta / E_r = \nu_\theta / \nu_r$. The stress resultants are given by

$$N_r = \int_{-h/2}^{h/2} \sigma^*_r \, dz = \frac{E_\theta h}{\beta - \nu_\theta^2} \left[u^*_{,r} - w^*_{0,r} w^*_{,r} + \frac{1}{2} w^{*2}_{,r} + \nu_\theta \frac{u^*}{r} \right]$$

$$N_\theta = \int_{-h/2}^{h/2} \sigma^*_\theta \, dz = \frac{E_\theta h}{\beta - \nu_\theta^2} \left[\nu_\theta \left(u^*_{,r} - w^*_{0,r} w^*_{,r} + \frac{1}{2} w^{*2}_{,r} \right) + \beta \frac{u^*}{r} \right] \tag{3}$$

$$M_r = \int_{-h/2}^{h/2} z \sigma^*_r \, dz = -D \left(w^*_{,rr} + \nu_\theta \frac{w^*_{,r}}{r} \right)$$

$$M_\theta = \int_{-h/2}^{h/2} z \sigma^*_\theta \, dz = -D \left(\nu_\theta w^*_{,rr} + \beta \frac{w^*_{,r}}{r} \right) \tag{4}$$

$$Q_r = \int_{-h/2}^{h/2} \sigma^*_{rz} \, dz$$

where $D = E_\theta h^3 / [12(\beta - \nu_\theta^2)]$.

Neglecting the damping and in-plane as well as rotary inertia and applying Hamilton's principle gives the differential equations of conical caps as

$$(rN_r)_{,r} - N_\theta = 0 \tag{5}$$

$$M_{\theta,r} - (rM_r)_{,rr} - [rN_r (w^* - w^*_0)_{,r}]_{,r} = (q - \gamma h w^*_{,tt}) \tag{6}$$

The condition of zero shear at the center is

$$-2\pi [(rM_r)_{,r} - M_\theta + rN_r (w^* - w^*_0)_{,r}] \big|_{r=0} = 0 \tag{7}$$

Equation (5) is satisfied if the stress resultants are expressed in terms of a stress function ψ^* as follows:

$$N_r = \psi^* / r, \qquad N_\theta = \psi^*_{,r} \tag{8}$$

Integrating Eq. (6) from 0 to r and using Eq. (7) gives

$$M_\theta - (rM_r)_{,r} - rN_r (w^* - w^*_0)_{,r} = \int_0^r (q - \gamma h w^*_{,tt}) r \, dr \tag{9}$$

Using Eqs. (1), (4), and (8), the equation of motion (9) can be expressed in terms of w^* and ψ^* as

$$r^2 w^*_{,rrr} + r w^*_{,rr} - \beta w^*_{,r} - \frac{r\psi^*}{D} \left(w^*_{,r} + \frac{H}{a} \right) = \frac{1}{D} \int_0^r (q - \gamma h w^*_{,tt}) r \, dr \tag{10}$$

Eliminating u^* from Eqs. (3) and using Eqs. (1) and (8), the compatibility equation can be expressed in terms of ψ^* as

$$r^2 \psi^*_{,rr} + r \psi^*_{,r} - \beta \psi^* + \frac{1}{2} r h E_\theta w^*_{,r} \left(w^*_{,r} + 2 \frac{H}{a} \right) = 0 \tag{11}$$

Then, introduce the following dimensionless parameters:

$$w = \frac{w^*}{h}, \qquad \psi = \frac{a}{D} \psi^*, \qquad \rho = \frac{r}{a}, \qquad \tau = \left[\frac{D}{\gamma h a^4} \right]^{1/2} t$$

$$Q = \frac{q}{p_{CL}} = \frac{1}{8} [3(1 - \nu^2)]^{1/2} \left(\frac{h}{H} \right)^2 \frac{q a^4}{E h^4} \tag{12}$$

where E = minimum of E_r, E_θ, ν = maximum of ν_r and ν_θ, and

$$p_{CL} = \frac{8}{[3(1 - \nu^2)]^{1/2}} \left(\frac{H}{h} \right)^2 \cdot \frac{E h^4}{a^4}$$

is the classical buckling pressure for a full isotropic spherical shell corresponding to a spherical cap of base radius a and apex rise H with Young's modulus E and Poisson's ratio ν. The governing equations (10) and (11) reduce to the following dimensionless form:

$$\rho^2 w''' + \rho w'' - \beta w' - \psi \rho \left(w' + \frac{H}{h} \right) = \rho \left\{ \int_0^\rho \left[\frac{96(\beta - \nu_\theta^2)}{[3(1 - \nu^2)]^{1/2}} \cdot \frac{E}{E_\theta} \left(\frac{H}{h} \right)^2 Q - \ddot{w} \right] \rho \, d\rho \right\} \tag{13}$$

$$\rho^2 \psi'' + \rho \psi' - \beta \psi + 6(\beta - \nu_\theta^2) \rho w' \left(w' + 2 \frac{H}{h} \right) = 0 \tag{14}$$

where $(\,)'$ and $(\dot{\,})$ are derivatives with respect to ρ and τ, respectively. The initial conditions are assumed to be

$$w(\rho, 0) = \dot{w}(\rho, 0) = 0 \tag{15}$$

The symmetry conditions at the center and the boundary conditions for caps with clamped immovable, simply supported immovable, and simply supported movable edges (Fig. 1) are

$\rho = 0$: $w' = 0, \ \psi = 0$ (16)

$\rho = 1$: $w = 0$ (17)

$w' = 0, \ \psi' - \nu_\theta \psi = 0$ (clamped immovable) (18a)

$w'' + \nu_\theta w' = 0, \ \psi' - \nu_\theta \psi = 0$ (simply supported immovable) (18b)

$w'' + \nu_\theta w' = 0, \ \psi = 0$ (simply supported movable) (18c)

Method of Solution

To obtain the transient response, the time is incremented in small steps $\Delta\tau$ and the nonlinear equations (13) and (14) are solved iteratively at each step J by linearizing the nonlinear terms for each iteration as

$$(w'\psi)_J = w'_{J_p} \psi_J, \qquad (w')^2_J = w'_{J_p} w'_J \tag{19}$$

where the predicted term w'_{J_p} is taken as the mean of its value at the two preceding iterations. For the first iteration, the predicted value w'_{J_p} is extrapolated quadratically from the values of w' at the three preceding steps,

$$w'_{J_p} = A_1 w'_{J-1} + A_2 w'_{J-2} + A_3 w'_{J-3} \tag{20}$$

where A_1, A_2, and A_3 for various steps are 1,0,0($J = 1$); 2, −1,0($J = 2$); and 3, −3,1($J \geq 3$).

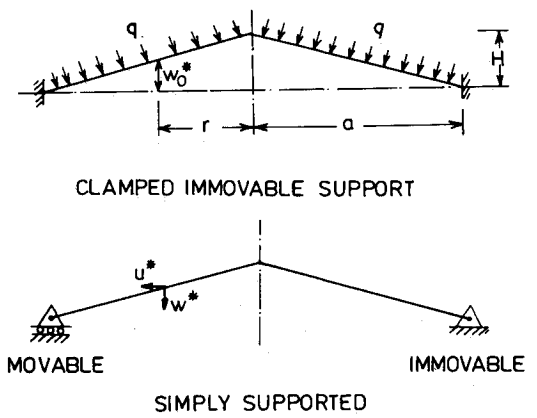

Fig. 1 Geometry and loading for conical cap.

The orthogonal point collocation method,[6] with the zeros of a Legendre polynomial as collocation points, has been used for the spatial discretization of Eqs. (13) and (14). For N collocation points, the deflection w and stress function ψ are expanded as finite degree polynomials in ρ

$$w(\rho)=\sum_{m=1}^{N+3}\rho^{m-1}a_m, \qquad \psi(\rho)=\sum_{n=1}^{N+2}\rho^{n-1}b_n \tag{21}$$

The N collocation points ρ_i are taken at the zeros of the Nth degree Legendre polynomial in a range of 0-1. The Newmark-β scheme[7] with the parameters corresponding to the average acceleration method is used to discretize the inertia term

$$\ddot{w}_J=\frac{4(w_J-w_{J-1})}{(\Delta\tau)^2}-\frac{4\dot{w}_{J-1}}{(\Delta\tau)}-\ddot{w}_{J-1} \tag{22}$$

The $2N$ collocation equations for the differential equations (13) and (14) are

$$\sum_{m=1}^{N+3}\left\{(m-1)\rho_i^{m-2}[(m-2)^2-\beta]+\frac{4}{(\Delta\tau)^2(m+1)}\rho_i^{m+2}\right\}a_m - \sum_{n=1}^{N+2}\left\{\left[(w'_{J_p})_i+\frac{H}{h}\right]\rho_i^n\right\}b_n=\frac{48(\beta-\nu_\theta^2)}{[3(1-\nu^2)]^{1/2}} \times\frac{E}{E_\theta}\left(\frac{H}{h}\right)^2\rho_i^3Q_J+\rho_i\int_0^{\rho_i}\left[\frac{4w}{(\Delta\tau)^2}+\frac{4\dot{w}}{(\Delta\tau)}+\ddot{w}\right]_{J-1}\rho\,d\rho \tag{23}$$

$$\sum_{m=1}^{N+3}\left\{6(\beta-\nu_\theta^2)\left[(w'_{J_p})_i+2\frac{H}{h}\right](m-1)\rho_i^{m-1}\right\}a_m + \sum_{n=1}^{N+2}\{\rho_i^{n-1}[(n-1)^2-\beta]\}b_n=0, \quad i=1\ldots,N \tag{24}$$

The five equations for the boundary conditions are solved for a_1,a_2,a_3 and b_1,b_2 in terms of the remaining Na's and Nb's, respectively. Equations (23) and (24) are the $2N$ discretized equations for these a's and b's. These are solved by Gaussian elimination with pivoting. The iterations are continued until the average deflection $\bar{w}$ converges within 0.1% accuracy. Convergence studies have revealed that nine collocation points and $\Delta\tau=0.001$-0.01 (depending on edge conditions, orthotropic parameter β, and shell parameter H/h) yield quite accurate converged results. As a further check on the accuracy of the results, at every step the sum of the kinetic and strain energies of the cap is compared with the sum of initial kinetic energy and the external work done up to that step. The difference between those two sets of energies has been found to be negligible at all steps.

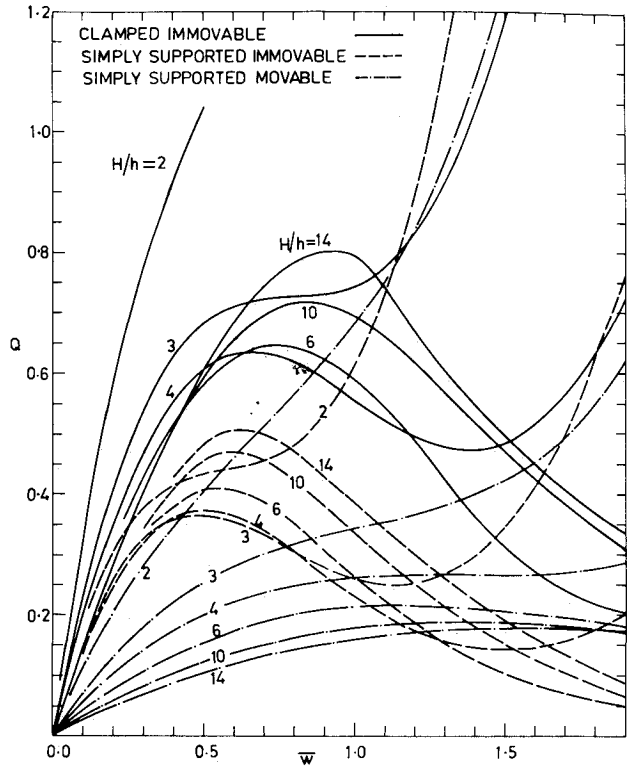

Fig. 2 Deflection response of conical caps under static load for $\beta=10$.

Buckling Criteria

Dynamic Buckling

The criterion suggested by Budiansky and Roth[8] is adopted in this study. The peak average displacement in the time history $\bar{w}_{max}$ of the cap is plotted against the magnitude of the step load, where the average displacement $\bar{w}$ is given by

$$\bar{w}=\int_0^a 2\pi rw\,dr\Big/\left(\int_0^a 2\pi r\,dr\right)=2\int_0^1 w\rho\,d\rho=2\left(\sum_{m=1}^{N+3}\frac{a_m}{m+1}\right) \tag{25}$$

In case there is a situation in which a distinct jump in $\bar{w}_{max}$ occurs with a small change in the load, this load is taken to be the dynamic buckling load. On the other hand, if there is a gradual transition from the low to the high range of $\bar{w}_{max}$, the buckling load is taken as that corresponding to the lower knee of the load vs $\bar{w}_{max}$ curve.[9,10]

Static Buckling

The average deflection $\bar{w}$ is incremented in small steps and the governing equations are solved to obtain the corresponding load at each step. If a maximum occurs in the value of the load, then it is taken as the static snap-through buckling load.

Dynamic Buckling Loads from Static Analysis

The computer time necessary for obtaining the dynamic buckling load using the forced vibration approach discussed above is very large. The "energy criterion" of Hoff and Bruce[11] provides a method to find dynamic buckling loads

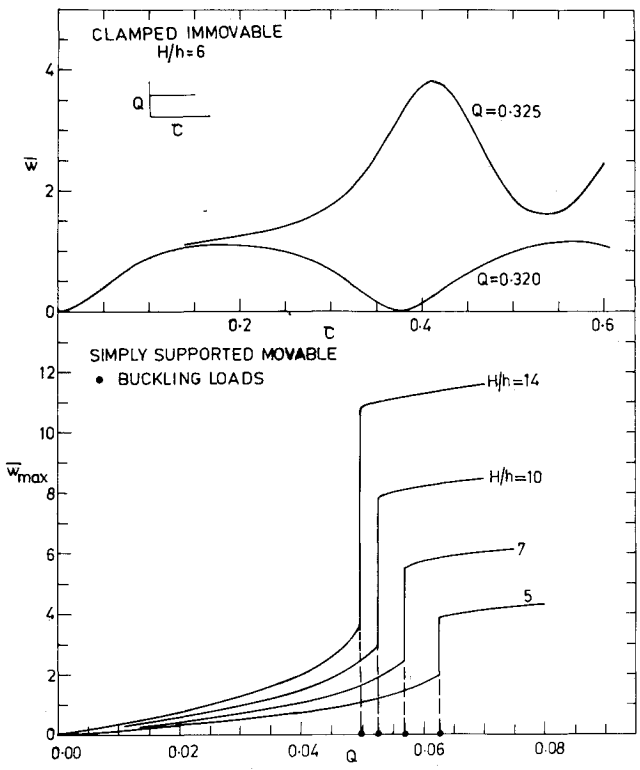

Fig. 3 Deflection response of conical caps under step loads ($\beta = 1$).

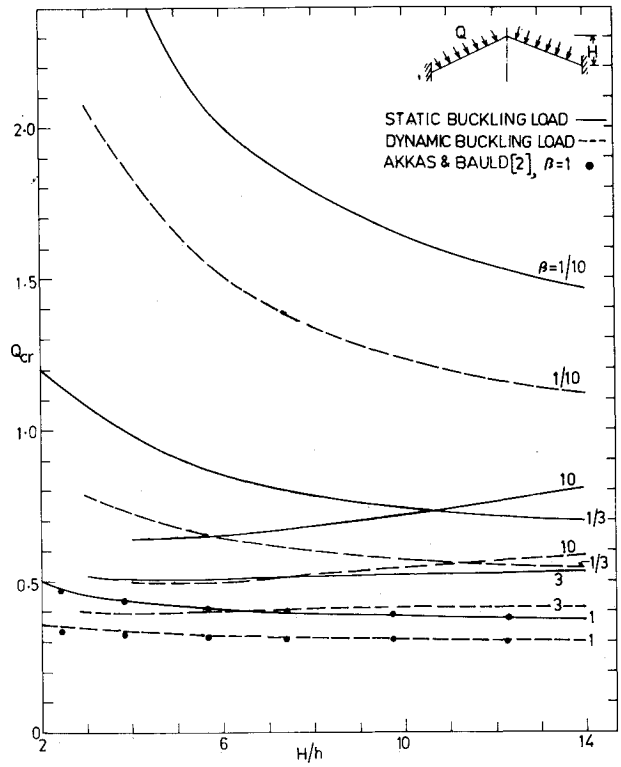

Fig. 4 Effect of β on buckling loads of clamped immovable caps.

Table 1 Effect of Poisson's ratio ν on static buckling load ($H/h = 8$)

	Q_{cr} Clamped immovable			Simply supported immovable			Simply supported movable		
ν	$\beta=1$	10	0.1	1	10	0.1	1	10	0.1
0.25	0.3843	0.6882	1.783	0.1892	0.4445	0.6378	0.06909	0.1973	0.2364
0.30	0.3927	0.6833	1.791	0.1945	0.4442	0.6415	0.07028	0.1959	0.2376
0.35	0.4021	0.6765	1.800	0.2002	0.4426	0.6455	0.07157	0.1940	0.2388

from static analysis. It is assumed that if the structure can reach an unstable static equilibrium configuration during its forced oscillations, it may then buckle. Using this method, sufficiently accurate dynamic loads for spherical caps have been obtained by Akkas.[12]

A similar criterion has been used in this study to determine dynamic buckling loads from static analysis. Approximate value of the maximum response $\bar{w}_{\max}$ under step loads is determined from static analysis. It is assumed that, at the instant of the maximum average deflection, the cap has zero velocity and the deflected shape is the same as that under a static load causing the same average deflection. If the uniformly distributed static load Q results in an average deflection $\bar{w}$ with the strain energy $U(Q)$, then the step load Q_0 that will yield the maximum average deflection $\bar{w}_{\max}$ equal to $\bar{w}$ is given by

$$\int_0^a w^*(r) q_0 2\pi r dr = \frac{16\pi}{[3(1-\nu^2)]^{1/2}} \left(\frac{H}{h}\right)^2 \frac{h^5}{a^2} E Q_0 \times \left(\sum_{m=1}^{N+3} \frac{a_m}{m+1}\right) = U(Q) \tag{26}$$

If $Q_0 = Q$, this load is taken as the dynamic buckling load by Akkas.[12] In the present study, the first maximum of the step load Q_0 vs $\bar{w}_{\max}$ curve obtained from the static analysis has been taken as the dynamic buckling load. This value happens to be the same as the one obtained using the criterion adopted by Akkas.

Results and Discussion

The influence of orthotropic parameter β and in-plane and rotational edge conditions at the support on the axisymmetric static and dynamic buckling loads of shallow conical caps subjected to uniformly distributed load has been investigated for several values of the apex rise-to-thickness ratio H/h. The response may be asymmetric for higher values of the rise parameter H/h and for some values of β. However, this investigation is limited to axisymmetric buckling. The effect of Poisson's ratio ν on the static buckling load of a conical cap, with rise parameter $H/h = 8$, is shown in Table 1 for three edge conditions and three values of the orthotropic parameter β. It is concluded from these results that the effect of Poisson's ratio ν is not significant. The larger Poisson's ratio ν has been taken as 0.3 in all of the remaining cases considered in this study.

The deflection response of conical caps with clamped immovable, simply supported immovable, and simply supported movable edges subjected to uniformly distributed static load is displayed in Fig. 2 for $\beta = 10$ and shell parameter $H/h = 2,3,4,6,10,14$. Caps with $H/h = 2$ do not snap through, but rather show the typical behavior of initial softening followed by hardening. The cap with $H/h = 3$

snaps through for the simply supported immovable case, but does not for the clamped immovable and simply supported movable cases. For the simply supported immovable cap with $H/h=3$, it has been possible to obtain portions of the response curve corresponding to unstable static equilibrium configurations as well as the postbuckling portion of the curve after snap-through. Caps with higher values of H/h snap through for all edge conditions. In all cases, the static buckling load is determined from the maxima in the load-deflection curve.

Typical average deflection responses to uniformly distributed step loads are shown in Fig. 3. The maximum average deflection has a sharp jump when the step load is increased from 0.320 to 0.325 for isotropic clamped immovable conical caps with $H/h=6$. Hence, the snap-through dynamic buckling load Q_{cr} lies between 0.320 and 0.325. Buckling loads have been obtained on the basis of a few cycles. More accurate buckling loads can be obtained by studying the transient response for a large number of cycles, but at the cost of greater computational time. The inevitable presence of damping tends to increase the dynamic buckling loads, as has been shown for spherical caps by Ganapathi and Vardan.[13] Thus, the dynamic buckling loads based on transient responses for a few cycles, although on the high side, are practically meaningful in the context of the inevitable presence of damping. The variation of the maximum average deflection with the load for isotropic simply supported immovable conical caps is shown in Fig. 3 for $H/h=5,7,10,14$. The dynamic buckling loads corresponding to a sharp jump in the maximum average deflection are also indicated. In almost all cases extending over a wide range of β, H/h, and boundary conditions, the dynamic buckling load has been found from a sharp jump in the maximum average deflection. In very few cases of $H/h=2$ or 3, it has been found from lower knee of the load vs $\bar{w}_{max}$ curve.

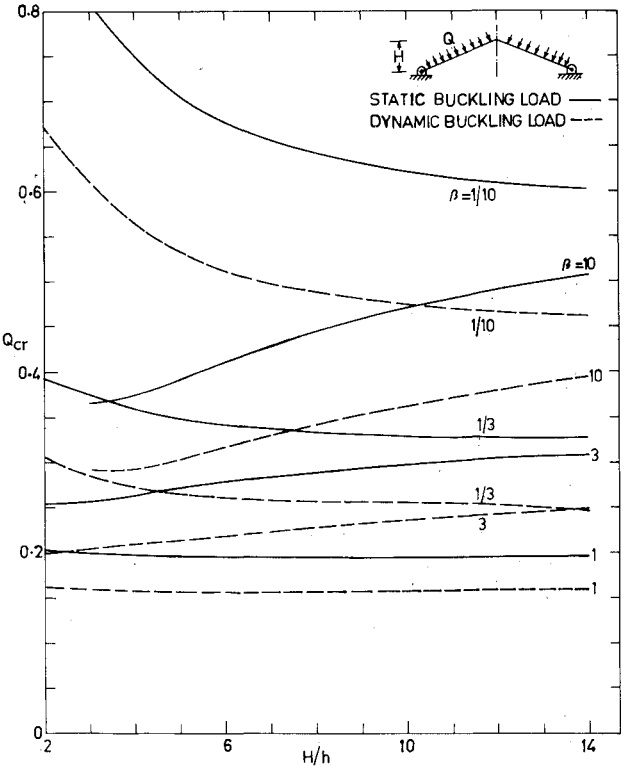

Fig. 5 Effect of β on buckling loads of simply supported immovable caps.

The effect of orthotropic parameter β on the static and dynamic buckling loads of conical caps with clamped immovable edges under uniformly distributed static and step function loads is depicted in Fig. 4. An isotropic case ($\beta=1$), two orthotropic cases with $\beta<1$ ($\beta=1/3,1/10$), and two orthotropic cases with $\beta>1$ ($\beta=3,10$) are considered. The present results for the isotropic case agree well with the results of Akkas and Bauld.[2] Being based on the transient response for a few cycles, the dynamic results are somewhat higher than those of Ref. 2. It is observed from Fig. 4 that the static and dynamic buckling loads increase with the degree of orthotropicity for $\beta<1$ as well as for $\beta>1$. The increase for β of less than 1 is greater than the corresponding increase for β of more than 1. The dimensionless buckling load Q_{cr} decreases with the rise in parameter H/h for $\beta=1$, 1/3, and 1/10 and increases with H/h for $\beta=3$ and 10. In all cases, the dynamic buckling load is about 80% of the static buckling load.

The effect of orthotropic parameter β on the buckling loads of conical caps with simply supported immovable edges is shown in Fig. 5. The buckling loads increase with the degree of orthotropicity. The effect of β and H/h on Q_{cr} is similar to the clamped immovable case. The buckling loads for the simply supported immovable caps are much smaller

Table 2 Comparison of dynamic buckling loads from static and transient analysis

		Q_{cr}					
		Clamped immovable		Simply supported immovable		Simply supported movable	
β	H/h	Static analysis	Dynamic analysis	Static analysis	Dynamic analysis	Static analysis	Dynamic analysis
1	6	0.3206	0.322	0.1557	0.1560	0.05906	0.0595
	10	0.3075	0.308	0.1564	0.1575	0.05246	0.0525
	14	0.2981	0.303	0.1583	0.1605	0.04956	0.0498
3	6	0.3941	0.397	0.2183	0.219	0.09362	0.0940
	10	0.4056	0.410	0.2337	0.237	0.08320	0.0834
	14	0.4048	0.415	0.2430	0.247	0.07868	0.0792
10	6	0.4959	0.497	0.3117	0.3175	0.1708	0.1688
	10	0.5242	0.547	0.3495	0.3625	0.1469	0.1472
	14	0.5364	0.583	0.3747	0.3935	0.1407	0.1407
1/3	6	0.6686	0.641	0.2731	0.2613	0.10224	0.0978
	10	0.5923	0.569	0.2651	0.2548	0.09197	0.0883
	14	0.5611	0.539	0.2638	0.2545	0.08715	0.0836
1/10	6	1.5412	1.507	0.5381	0.5113	0.1905	0.1834
	10	1.2861	1.234	0.4953	0.4747	0.1721	0.1669
	14	1.1604	1.118	0.4815	0.4613	0.1658	0.1579

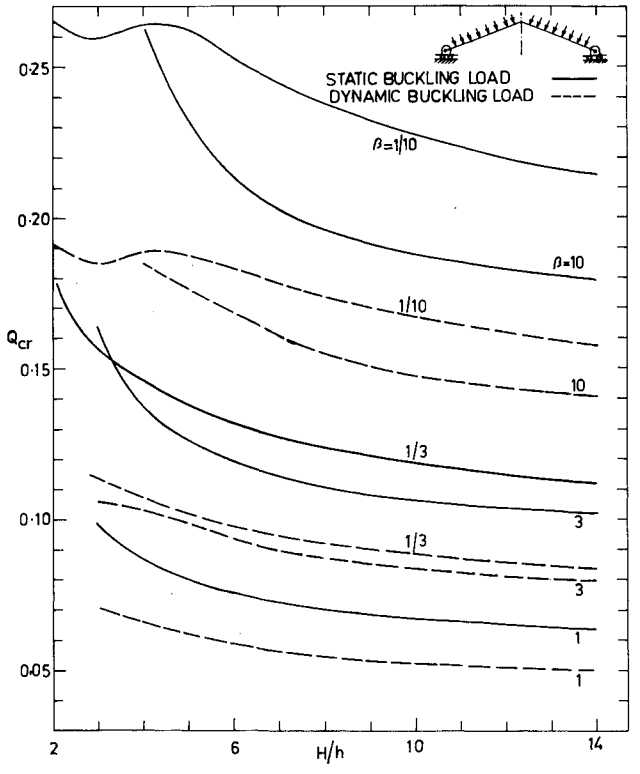

Fig. 6 Effect of β on buckling loads of simply supported movable caps.

than those for the clamped immovable caps, implying that the rotational edge condition has a significant effect on the buckling loads.

The effect of orthotropic parameter β on the buckling loads of conical caps with simply supported movable edges is presented in Fig. 6. The buckling loads increase with the degree of orthotropicity. The increase is again more pronounced for $\beta<1$ than for $\beta>1$. In general, the buckling load Q_{cr} decreases with H/h for this case. The buckling loads for simply supported movable caps are much smaller than those for the simply supported immovable caps, indicating the strong influence of the in-plane edge conditions on the buckling loads.

The uniformly distributed dynamic buckling loads obtained from static analysis are compared with those obtained from transient analysis in Table 2. It can be seen that sufficiently accurate values of the dynamic buckling loads can, for practical purposes, be obtained from static analysis over a wide range of the edge condition, orthotropic parameter, and shell parameter H/h. Thus, the applicability of the method of determining dynamic buckling loads from static analysis has been demonstrated for the structural configuration of a shallow conical cap.

Conclusions

The axisymmetric buckling of orthotropic shallow conical caps subjected to uniformly distributed static and step function loads has been studied. Marguerre-type governing equations have been discretized spatially by the orthogonal point collocation method and temporally by the Newmark-β scheme. The effect of Poisson's ratio ν has been found to be marginal. The buckling loads increase with the degree of orthotropicity for $\beta<1$ as well as for $\beta>1$. The increase is greater for $\beta<1$ than for $\beta>1$. The dynamic buckling loads are about 80% of the static buckling loads. The in-plane and rotational edge conditions have been found to have a significant influence on the buckling loads. Sufficiently accurate dynamic buckling loads have been obtained from static analysis. Thus, the validity of this economical method of determining dynamic buckling loads for the case of shallow conical caps is demonstrated.

Acknowledgments

The authors gratefully acknowledge the constructive suggestions of the two reviewers of this paper.

References

[1]Fung, Y. C. and Sechler, E. E., *Thin Shell Structures: Theory, Experiment and Design*, Prentice-Hall, Englewood Cliffs, NJ, 1970.

[2]Akkas, N. and Bauld, N. R. Jr., "Axisymmetric Dynamic Buckling of Clamped Shallow Spherical and Conical Shells under Step Load," *AIAA Journal*, Vol. 8, 1970, pp. 2276-2277.

[3]Akkas, N. and Bauld, N. R. Jr., "Static and Dynamic Buckling Behaviour of Clamped and Shallow Conical Shells," *International Journal of Mechanical Sciences*, Vol. 13, 1971, pp. 689-706.

[4]Hubner, W. and Emmerling, F. A., "Axialsymmetrische grobe Deformation einer elastischen Kegelschale," *Zeitschrift fuer Angewandte Mathematik und Mechanik*, Vol. 62, 1982, pp. 408-411.

[5]Hubner, W., "Deformationen und Spannungen bei Tellerfedern," *Konstruktion*, Vol. 34, 1982, pp. 387-392.

[6]Villadsen, J. V. and Michelsen, M. L., *Solution of Differential Equation Models by Polynomial Approximation*, Prentice-Hall, Englewood Cliffs, NJ, 1978.

[7]Bathe, K. J. and Wilson, E. L., *Numerical Methods in Finite Element Analysis*, Prentice-Hall, Englewood Cliffs, NJ, 1976.

[8]Budiansky, B. and Roth, R. S., "Axisymmetric Dynamic Buckling of Clamped Shallow Spherical Shells," NASA TN D151, 1962, pp. 597-606.

[9]Stephens, W. B. and Fulton, R. E., "Axisymmetric Static and Dynamic Buckling of Spherical Caps Due to Centrally Distributed Pressure," *AIAA Journal*, Vol. 7, Nov. 1969, pp. 2120-2126.

[10]Kao, R. and Perrone, N., "Dynamic Buckling of Axisymmetric Spherical Caps with Initial Imperfections," *Computers and Structures*, Vol. 9, No. 5, 1978, pp. 463-473.

[11]Hoff, N. J. and Bruce, V. G., "Dynamic Analysis of the Buckling of Laterally Loaded Flat Arches," *Journal of Mathematics and Physics*, Vol. 32, 1954, pp. 276-288.

[12]Akkas, N., "Note on the Dynamic Buckling Loads of Shallow Spherical Shells from Static Analysis," *Journal of Structural Mechanics*, Vol. 9, No. 4, 1981, pp. 483-488.

[13]Ganapathi, M. and Vardan, T. K., "Dynamic Buckling of Orthotropic Shallow Spherical Shells," *Computers and Structures*, Vol. 15, No. 5, 1982, pp. 517-520.